

## 14A.4 MOBILE X-BAND DUAL POLARIZATION PHASED ARRAY RADAR: SYSTEM REQUIREMENTS AND DEVELOPMENT

K. Orzel \*, V. Venkatesh, R. Palumbo, R. Medina, J. Salazar, A. Krishnamurthy,  
E. Knapp, D. McLaughlin, R. Tessier, S. Frasier  
University of Massachusetts, Amherst, USA

**Abstract**—This paper describes the X-band dual polarization phased array radar being developed at the University of Massachusetts. The high level system architecture is presented. The scanning strategy as well as pulse compressor design considerations are discussed.

**Index Terms**—phased array, dual polarization, weather radar

### 1. INTRODUCTION

The recently implemented upgrade of WSR-88D radar network to a dual polarization capability is a direct consequence of almost two decades of research that has shown that additional polarization can significantly increase the amount of information delivered by weather radar systems. On the other hand, one still unresolved bottleneck of a current meteorological radar system is low temporal resolution. Long revisit time on order of 5 min reduces the chance to observe quickly evolving phenomena such as tornadoes as well as issuing accurate warnings in advance. It is believed that electronically scanned antennas pose a solution to solve this restriction, but due to the high cost of narrow beam phased arrays, their implementation in weather sensing radar remains very limited. The Microwave Remote Sensing Laboratory (MIRSL) at the University of Massachusetts is currently designing a novel low cost X-band radar which will be the first mobile, dual polarization phased-array system developed for meteorological applications.

### 2. SYSTEM OVERVIEW

The MIRSL Phased Array Radar block diagram is shown in Figure 1. The system consists of the Phase-Tilt Antenna, Up/Down Converter, IF Digital Transceiver, Host Computer, Pedestal and Array Controller/Formatter. The Phase Tilt Antenna subsystem was designed at the Center for Collaborative Adaptive Sensing of the Atmosphere (CASA) for use in distributed, collaborative and adaptive sensing networks (Hopf et al. 2009). It is a one dimensional dual-polarization active array antenna that enables electronic scanning in the azimuth plane, while scanning in the elevation plane is performed mechanically. This type of antenna architecture reduces the number of required T/R modules and hence significantly decreases the overall system cost.

Furthermore, the antenna subsystem is a modular design composed of four line replaceable units (LRU). This design approach is an attempt to facilitate future system extensions.

A FPGA based Array Controller/Formatter provides control and timing signals for all subsystems (with the exception of pedestal). Owing to low peak power provided by solid state based T/R modules, implementation of pulse compression techniques is required. The transmitted nonlinear chirp is produced by an arbitrary waveform generator within the digital IF transceiver and is compressed by means of an inverse filter. The host computer generates all scanning settings, executes signal processing and controls the data flow.

#### 2.1 Phase-Tilt Antenna Subsystem

Each LRU consists of a 0.27 x 0.56 m passive antenna array, a set of 16 T/R modules and a DC and signal distribution backplane. The linear array is a planar structure of 72 columns. The central 64 columns of the antenna array are fed by dedicated T/R modules, while the remaining 8 outer columns are used as terminated dummy elements in order to reduce the effects of diffraction and non-uniform mutual coupling (Knapp et al. 2011). Each column is a dual linear polarized subarray composed of 32 aperture coupled microstrip patch antennas interconnected by series-fed networks for each

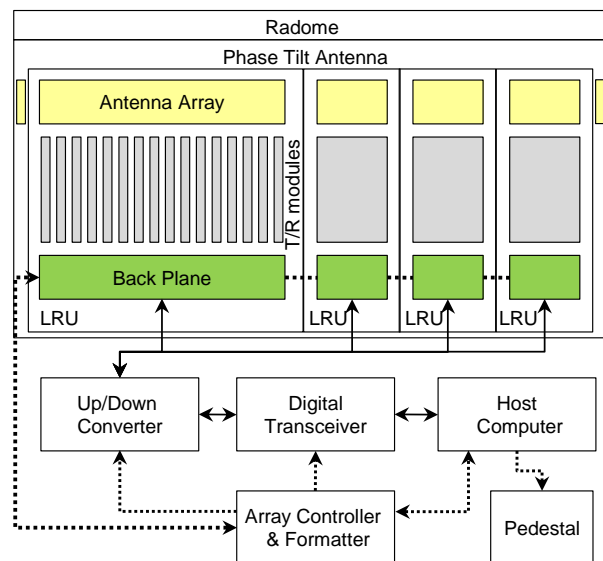


Fig. 1: Phased array radar block diagram and signal flow.

\* Corresponding author address: Krzysztof Orzel, University of Massachusetts, Department of Electrical and Computer Engineering, Amherst, MA 01003; email: korzel@engin.umass.edu

polarization. Here, two serpentine lines are implemented to feed each radiating element in both polarizations. Although a series feed compared to its corporate alternative, exhibits lower transmission loss and require less substrate area, its performance is frequency dependent, which limits antenna bandwidth.

The phase tilt antenna allows scanning of  $\pm 45^\circ$  in the horizontal plane with a beam width of  $3.5^\circ$  in elevation and  $2^\circ$  in azimuth at broadside. It is also important to highlight that in case of dual polarized phased arrays, removing biases due to the coupling of H and V fields exhibits a great challenge, since the antenna radiation patterns depend on the pointing direction. Wang and Chandrasekar (2006) reported that cross-polarization isolation in excess of  $-20$  dB is required to maintain measured bias error in differential reflectivity below  $0.1$  dB. The first prototype of CASA phase tilt antenna described by Salazar et al. (2010) meets this requirement. The cross-polarization isolation of  $-35$  dB and  $-32$  dB at broadside for V and H respectively was measured in the frequency range between  $9.3$  GHz to  $9.4$  GHz. Furthermore if these values are integrated across entire scanning range of  $90^\circ$ , cross polarization better than  $-21$  dB is obtained for both channels.

A block diagram of a T/R module is presented in Figure 2. The T/R module architecture can be broken down into four sets of components: control block, diversity switch, transmit and receive channels. Operation of each individual T/R module is controlled by an independent FPGA, which can be accessed and programmed by array formatter. A custom-designed high-power, four-port diversity switch is a star configuration of four GaAs SPST (single pole, single throw) PIN diode switches. It is characterized by an insertion loss less than  $3$  dB and isolation in excess of  $45$  dB over the frequency band  $9$  to  $9.6$  GHz. This design approach allows calculation of all polarimetric products, but also forces alternate transmit alternate receive (ATAR) mode of operation. The transmitter block consists of a high and medium power amplifier. The transmit peak power is about  $1.25$  W. The receiver block consists of low noise amplifier and a gain block. The T/R modules design utilizes a “Common Leg” architecture (Medina et al. 2010)

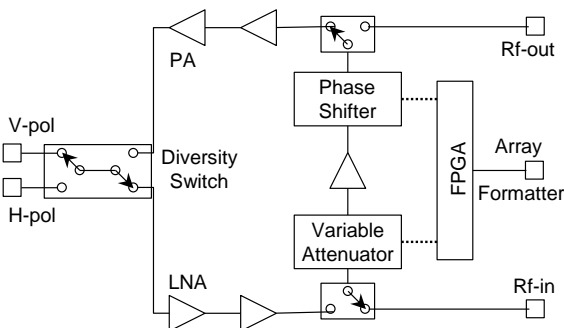


Fig. 2: T/R module block diagram

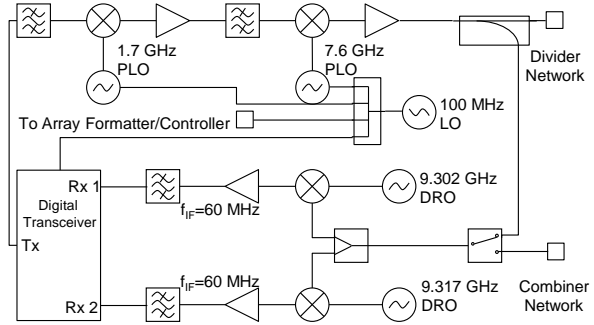


Fig. 3: RF subsystem block diagram.

ie phase shifter, gain block and variable attenuator are shared between transmit and receive channels. This configuration features  $360^\circ$  of phase control with  $5.6^\circ$  of resolution and  $31.5$  dB of amplitude control with  $0.5$  dB of resolution. The common part of the circuit is connected to the independent input and output ports by means of two T/R switches.

Each LRU backplane is used as an interface between T/R modules and the remainder of the system. The backplane provides DC power distribution and a  $25$  MHz low voltage differential signals bus for fast programming and communication to the T/R modules.

## 2.2 RF Subsystem

Figure 3 shows a block diagram of the RF subsystem. It consists of a double stage up-converter, which provides LO rejection as well as suppression of harmonics and spurious signals (over  $48$  dB) in frequency range between  $9.2$  and  $9.5$  GHz. A calibration loop for an X-band signal can be used during field calibration. It also enables recording of the transmitted frequency modulated waveform. This feature is particularly beneficial if inverse filter is used for pulse compression. The filter design based on the calibration data will result in reduced range sidelobe levels.

A dual-channel down-converter is implemented in single stage configuration. The second channel can be used to cover a blind zone due to transmission of long chirp at no penalty in scanning time. Alternatively, frequency hopping techniques can be used to increase the number of independent samples.

## 2.3 Timing Control Subsystem

A core component of phased array radar is the array formatter. It is a FPGA-based master controller that translates user commands from the host computer to control and timing signals for the radar system. The array formatter loads look-up tables and sequence table for all T/R modules.

The look-up table contains the calibration values that have to be set for phase shifter and variable attenuator in order to switch to the requested beam location. The look-up table defines up to  $256$  beam positions in four operation modes (TxV, TxH, RxV, RxH). These settings are independent for each T/R module and are stored in its

internal nonvolatile memory. The array formatter updates this memory each time the system calibration is modified due to the external environment.

At the beginning of a PPI scan a host computer uploads all azimuth beam positions into an array formatter memory. Then for each beam position a sequence table is created, which is updated on beam to beam basis. Sequence table contains the timing data and beam IDs that are required to configure state machines in each T/R module. Since the sequence table holds only register addresses, the array formatter broadcasts single sequence table simultaneously to all T/R modules. Therefore the beam switching time is reduced to 100  $\mu$ s. Finally, the host computer verifies that all data have been successfully received, actuates pedestal elevation position and starts new scan.

## 2.4 Data Acquisition Subsystem

The data acquisition subsystem consists of a high speed digital transceiver, PC based signal processor and a RAID for data storage. A commercial digital transceiver (Pentek 7140) is integrated into the host computer and serves as an arbitrary waveform generator and a data digitizer. The transmitted waveform is synthesized at intermediate frequency range between 62 and 77 MHz. On board 14-bit A/D converters sample each IF receiver channel at 100 MHz rate. The resulting sampled IF signals alias to an apparent intermediate frequency of 40 MHz. Then a digital complex mixer translates the real input signal down to complex baseband representation. Finally the signal is filtered and decimated resulting in a 16 bit in-phase and quadrature samples at 6.25 MHz sampling rate. The 14-bit A/D converters provide 78 dB of dynamic range, which is sufficient for a short range X-band weather radar system.

At this point the data are either streamed directly in a raw format tagged with beam ID and time to disk or to a signal processor. The data processing routine is based on a multithreading model, which allows truly concurrent execution of threads if multi-core processors are available. In order to prevent common data from being simultaneously modified by independent threads a set of semaphores is implemented to lock and unlock memory resources. The host computer provides real-time FFT-based pulse compressor. Also enables an accumulation of various covariance-based products over a specified number of pulses for up to 8 beam locations at a time if beam multiplexing methods are used.

## 3. PULSE COMPRESSOR DESIGN

Considering the losses of the cables between T/R modules and antenna feed network as well as the array antenna efficiency, the phase tilt antenna can deliver a maximum peak power of 50 W. Pulse compression is a signal processing technique, which overcomes low power limitation of solid state amplifiers and improves both radar sensitivity and range resolution at the same time. An optimal design of a radar waveform and pulse compression filter is a resultant of many mutually dependent factors. In view of the fact that the range resolution is almost at all

times several times finer than the azimuth resolution, a common procedure is to average few range samples together. For pulse compressed system range resolution can be well below 100 m, while azimuth resolution at 10 km will be 350m (at broadside), hence range gates averaging should be implemented. In that manner the accuracy of measurements can be improved, while the dwell time will be reduced. On the other hand, since deep reduction of range side lobes should be of a primary interest, implementation of side lobe suppression filter is necessary. Typically, such a filter will broaden the main lobe of compressed pulse and will also reduce signal to noise ratio (SNR) compared to the matched filter output.

In general, the FM waveform is superior to the Barker based phase coding, due to its satisfactory Doppler sensitivity and mismatch loss. Additionally, nonlinear frequency modulation (NLFM) waveform compared to their LFM counterparts exhibit small SNR reduction if range side lobe suppression filter is implemented. This is mainly due to the shape of power spectrum, which in case of NLFM chirp is less rectangular. Ashe et al. (1994) has shown that the tangent based NLFM waveform exhibits the best performance in terms of integrated sidelobe levels and mismatch losses if inverse filter is applied. The frequency progression is defined as follows:

$$f(t) = \pm B \frac{\tan(2\beta t/T)}{2\alpha} \quad \frac{T}{2} \leq t \leq \frac{T}{2}$$

$$\beta = \tan^{-1}(\alpha) \quad (1)$$

where + and - denote up- and down- chirp respectively,  $\alpha$  is a nonlinearity coefficient. Note that if  $\alpha \rightarrow 0$ , then (1) defines LFM waveform. The complex envelope of the NLFM waveform at baseband in terms of amplitude and phase modulation can be then expressed as:

$$u(t) = w(t) \cdot e^{j\pi f t} \quad \frac{T}{2} \leq t \leq \frac{T}{2} \quad (2)$$

where  $w(t)$  defines an amplitude modulation, which is used in order to reduce spectral leakage and Gibbs phenomenon. A good candidate for amplitude modulation is a Tukey window, which tapers the edges of transmitted waveform and forces that signal starts and ends at zero. In this manner the signal periodicity requirement for FFT processing is fulfilled. Additionally, application of window on transmit reduces signal bandwidth and in consequence undesired aliasing effect.

Inverse filter also known as Wiener filter is an optimal design that minimizes energy in sidelobes in the least square sense. As distinct from window based filter, an inverse filter is a unique design for a given waveform. It takes into account all nonlinearities in the spectrum of the transmitted signal and hence very low side lobes can be obtained at a minor reduction in SNR and range resolution. To compute filter coefficients we used the least-square error method described by Treitel et al (1966). The desired range resolution and sidelobe reduction level has been obtained by means of an iterative manner using a Nelder-Mead algorithm. The designed waveform is summarized in the Table 1.

TABLE 1. PULSE COMPRESSOR SPECIFICATIONS

Pulse length	20 $\mu$ sec
Waveform bandwidth	3 MHz
Receiver bandwidth	5 MHz
Sampling frequency	6.25 MHz
Frequency modulation	$\alpha = 1.0$
6dB mainlobe width	70 m
Filter length	200 taps
ISL within Doppler range $\pm 50$ m/s	$> 60$ dB
Worst case mismatch loss	0.8 dB

#### 4. SCANNING STRATEGY

In the traditional mechanically actuated weather radar, the scanning strategy is mostly dictated by a pedestal rotation speed and transmitter duty cycle. These limitations do not apply to phased array radar with solid-state transmitters. It will offer a great flexibility in scanning strategy and ultimately will adapt to the observed weather conditions. Therefore it is rather impractical to define a unique scanning pattern. There are certainly many different ways to provide dual polarization mode of operation, but a straightforward one is presented in Fig. 4. The Doppler velocity is estimated using vertically polarized pulse pair.

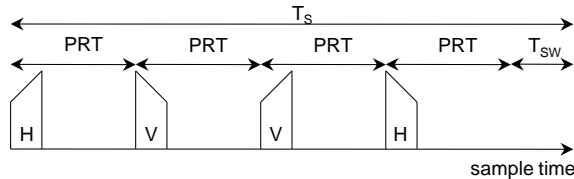


Fig. 4: Dual polarization pulsing scheme.

We suggest an alternate transmission of up- and down-chirps, which provides around 20 dB of second-trip echo rejection. Additional suppression of this signal contamination is achieved by polarization diversity. A pulse repetition frequency ( $PRF = 1/PRT$ ) of 5 kHz results in unambiguous range of 30 km and unambiguous velocity of  $\pm 37.5$  m/s, which is sufficient for most weather targets. To cope with higher wind velocities, the staggered PRT techniques can be implemented.

A PRF of 5 kHz may result in highly correlated weather samples. While this is desired for Doppler velocity estimation, an averaging of several pulses will not result in significant reduction of measurement errors. In order to collect independent pairs of samples beam multiplexing techniques are considered (Yu et al. 2006). For X-band radar the revisit time should be larger than 7 ms for spectrum widths larger than 1 m/s. Also, the angular separation of  $8^\circ$  between two successive beam locations is required to suppress the second-trip echoes from the previous beam locations by over 30 dB. The azimuth beam multiplexing pattern (BMX) is shown in Fig. 5. The BMX consists of 8 angular locations with  $2^\circ$  spacing. The first 4 pulses (see Fig. 4) are transmitted at  $a_1$ . Then the next sequence is transmitted at  $a_5$ , which is  $8^\circ$  from the first beam location and so on. As a result the radar is multiplexed over 8 beam locations. If pulses are separated by 200  $\mu$ s and beam switching time  $T_{sw}$  is 100  $\mu$ s, it takes

7.2 ms to scan all 8 locations. Hence the independence of subsequent pulse pairs is ensured.

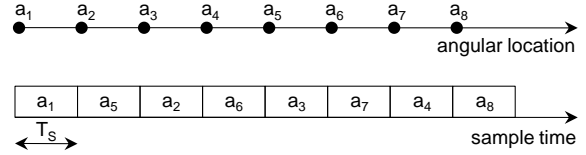


Fig. 5: An azimuth beam multiplexing pattern.

#### 5. SUMMARY

A dual-polarized, low-cost, solid-state X-band radar has been described. The key subsystems have been discussed in detail. A first prototype of CASA phase tilt antenna promises adequate performance for dual polarization weather applications providing cross-polarization isolation lower than 25 dB in the overall scanning range for both polarizations. The inverse filter based pulse compressor offers significant range sidelobe suppression and fine range resolution at a minor reduction in signal to noise ratio. An example of scanning strategy has been presented. Additionally, this radar will serve as a proof of transverse winds measurements using spaced antenna configuration.

#### ACKNOWLEDGMENTS

This work was supported by NSF Grant AGS-0937768 to the University of Massachusetts and by the Engineering Research Centers Program of the NSF under Award Number 0313747 to the CASA. Any opinions, findings, conclusions, or recommendations expressed in this material are those of the authors and do not necessarily reflect those of the NSF.

#### REFERENCES

- Ashe, J.M., R.L. Nevin, D.J. Murrow, H. Urkowitz, N.J. Bucci, and J.D. Nesper, 1994: Range Sidelobe Suppression of Expanded/Compressed Pulses with Droop. *IEEE International Radar Conference, Atlanta, GA*, 116-122.
- Hopf, A.P., J.L. Salazar, R.H. Medina, V. Venkatesh, E.J. Knapp, S. Frasier, and D.J. McLaughlin, 2009: CASA Phased Array System Description, Simulation and Products. *In Proceedings of IGARSS 2009*, 968-971.
- Knapp, E.J., J.L. Salazar, R.H. Medina, A. Krishnamurthy, and R. Tessier, 2011: Phase-Tilt Radar Antenna Array. *Proceedings of European Radar Conference 2011*.
- Medina, R.H., E.J. Knapp, J.L. Salazar, A.P. Hopf, and D.J. McLaughlin, 2010: T/R Module for CASA Phase-Tilt Radar Antenna Array. *IEEE International Symposium on Phased Array Systems & Technology*.
- Salazar, J.L., E.J. Knapp, and D.J. McLaughlin, 2010: Dual-polarization performance of the phase-tilt antenna array in a CASA dense network radar. *Proceedings of IGARSS 2010*, 3470-3473.
- Treitel, S., and E.A. Robinson, 1966: The design of high-resolution digital filters. *IEEE Transactions on Geoscience Electronics*, Vol. 4, No. 1, 25-38.
- Wang, Y., and V. Chandrasekar, 2006: Polarization Isolation Requirements for Linear Dual-Polarization Weather Radar in Simultaneous Transmission Mode of Operation. *IEEE Transactions on Geoscience and Remote Sensing*, Vol. 44, No. 0.
- Yu, T., M.B. Orescanin, C. Curtis, D.S. Zrnić, and D.E. Forsyth, 2006: Beam Multiplexing Using the Phased-Array Weather Radar. *Journal of Atmospheric and Oceanic Technology*, Vol. 24, 616 – 627.